

Expression of folate receptors in nasopharyngeal and laryngeal carcinoma and folate receptor-mediated endocytosis by molecular targeted nanomedicine

M Xie
H Zhang
Y Xu
T Liu
S Chen
J Wang
T Zhang

Department of Otorhinolaryngology
Head and Neck Surgery, Zhujiang
Hospital, Southern Medical University,
Guangzhou, People's Republic
of China

Abstract: Immunohistochemistry and an immunofluorescence technique was used to detect folate receptor expression in tissue samples and cell lines of head and neck squamous carcinoma, including 20 tissue samples of nasopharyngeal carcinoma, 16 tissue samples of laryngeal carcinoma, and HNE-1, HNE-2, CNE-1, CNE-2, SUNE-1, 5-8F, and Hep-2 cell lines. Iron staining, electron microscopy, and magnetic resonance imaging were used to observe endocytosis of folate-conjugated cisplatin-loaded magnetic nanoparticles (CDDP-FA-ASA-MNP) in cultured cells and transplanted tumors. As shown by immunohistochemistry, 83.3% (30/36) of the head and neck squamous carcinomas expressed the folate receptor versus none in the control group (0/24). Only the HNE-1 and Hep-2 cell lines expressed the folate receptor, and the other five cell lines did not. Endocytosis of CDDP-FA-ASA-MNP was seen in HNE-1 and Hep-2 cells by iron staining and electron microscopy. A similar result was seen in transplanted tumors in nude mice. Magnetic resonance imaging showed low signal intensity of HNE-1 cells and HNE-1 transplanted tumors on T2-weighted images after uptake of CDDP-FA-ASA-MNP, and this was not seen in CNE-2 transplanted tumors. In conclusion, head and neck squamous carcinoma cell strongly expressed the folate receptor, while normal tissue did not. The folate receptor can mediate endocytosis of folate-conjugated anticancer nanomedicines, and lays the foundation for molecular targeted treatment of cancer.

Keywords: nasopharyngeal carcinoma, laryngeal carcinoma, folate receptor, molecular targeting, cisplatin, nanomedicine

Introduction

Most head and neck cancers are squamous cell carcinomas. In view of their high metastatic potential, chemotherapy has become one of the main treatments in recent years, especially for laryngeal and nasopharyngeal carcinomas. Due to their lack of selectivity in tumor tissue, chemotherapeutic agents sometimes have severe side effects which may limit efficacy and induce drug resistance. The current study shows that targeted drug delivery by some proteins generally overexpressed on the surface of tumor cells can limit toxicity and improve the efficacy of cancer therapy.

Finding a specific molecular target for squamous cell carcinomas of the head and neck would contribute to the development of molecular targeted chemotherapy for these cancers. Specific molecular markers for nasopharyngeal and laryngeal carcinomas has not been found so far. The folate receptor (FR) is a glycosylphosphatidylinositol-anchored cell surface receptor that mediates folate transport into cells, and has three

Correspondence: Minqiang Xie
Department of Otorhinolaryngology
Head and Neck Surgery, Zhujiang
Hospital, Southern Medical University,
Guangzhou 510282, People's
Republic of China
Tel 86-20-61643389
Fax 86-20-61643010
Email min_qiang_x@hotmail.com

isomers (subtypes), ie, FR- α , FR- β , and FR- γ . The FR is rarely expressed in normal tissues,^{1,2} is highly expressed in breast cancer, endometrial cancer, nonmucinous ovarian adenocarcinoma, lung cancer, kidney cancer, and pancreatic cancer, and is known as a tumor-associated antigen.³⁻⁶ Folic acid (FA) is a water-soluble B vitamin, and is used in cells to synthesize thymine, which is critical for DNA synthesis, methylation, and repair. Folic acid is small (441 Da), stable over a broad range of temperatures and pH values, inexpensive, and nonimmunogenic. This molecule has high affinity for the FR, and can be transported into cells by FR-mediated endocytosis. Most importantly, it retains its ability to bind to the folate receptor after conjugation with other drugs.⁷ Because of this feature, the FR appears to be a promising molecular target for cancer therapy. After FA attaches to receptors located within the caveolae, it is internalized through the endocytic pathway. As the pH of the endosome approaches 5, FA dissociates from the receptor and the drug is released.

Recent studies have found that FA derivatives can be used in targeted imaging. Researchers prepared ⁶⁸Ga-NODAGA-folate conjugates for magnetic resonance imaging (MRI) and FA derivatives labeled with fluorine-18 for imaging by positron emission tomography. These targeted imaging reagents produced ideal contrast imaging in FR-positive KB (mouth epidermal carcinoma) cells and xenograft tumors in nude mice. Further, this molecular targeted effect could be blocked by preinjected free FA.⁸⁻¹⁰ Some studies have linked a gene vector with FA and have made targeted gene vectors, such as FA-1-palmitoyl-2-oleoyl-sn-glycero-3-ethylphosphocholine-cholesterol and FA-poly(ethylene glycol)-polyethylenimine.^{11,12} Compared with nontargeted carriers, these new vectors can improve the gene transfection efficiency of FR-positive HEK 293T cells, C6 cells, and KB cells *in vitro*,^{11,12} and have had stronger antitumor effects in experiments *in vivo*.¹³ Chemotherapeutic drugs (eg, paclitaxel, doxorubicin) conjugated with FA have been shown not only to be selectively transported into KB cells,^{14,15} Bel 7402 cells,¹⁶ and nude mice xenograft tumors, but also to achieve better antitumor results. Saba et al detected the FR in 45% of primary squamous cell carcinomas of the head and neck and 40% of corresponding lymph node metastases.¹³ Ward et al made acetylated generation 5 dendrimers conjugated with FA and methotrexate as the therapeutic moiety in compound reagents and administered them to nude mice with UM-SCC-1, UM-SCC-17B, and UM-SCC-22B cancer xenografts.¹⁷ They found this targeted therapy could be delivered in molar doses three times that of the free drug and with lower systemic toxicity.

In this study, we used immunohistochemistry and immunofluorescence techniques to detect FR expression in tissue samples and cell lines of nasopharyngeal and laryngeal carcinoma, and used iron staining, electron microscopy, and MRI to observe endocytosis of folate-conjugated cisplatin-loaded magnetic nanomedicines (CDDP-FA-ASA-MNP) in cultured cells and transplanted tumors. We investigated the molecular targeting of squamous cell carcinomas of the head and neck using folate-conjugated magnetic nanomedicines, and laid the foundation for development of FR-mediated targeted anticancer drugs.

Materials and methods

Cells and major reagents

Cells line for human nasopharyngeal carcinoma (HNE-1, HNE-2, CNE-1, CNE-2, SUNE-1, and 5-8F) were preserved by our laboratory. BALB/c nude mice (specific pathogen-free grade) were purchased from the Animal Experiment Center of Southern Medical University. Cell culture plates, microporous membranes (Corning Inc, New York, NY, USA), RPMI-1640 culture solution without folic acid (Gibco Grand Island, NY, USA), mouse antifolate binding protein antibody (LK26, Abcam Inc, Cambridge, MA, USA) were also purchased, and the CDDP-FA-ASA-MNP were prepared as we have previously reported.¹⁸ The mean diameter of the ferrous-ferric oxide (Fe₃O₄) core was 8.116 ± 0.24 nm, the hydrodynamic diameter was 110.9 ± 1.7 nm, and the zeta potential was -26.45 ± 1.26 mV. Maximum saturation magnetization was 22.2 emu/g. The encapsulation efficiency of cisplatin was $49.05\% \pm 1.58\%$ (mg/mL) and drug loading was $14.31\% \pm 0.49\%$ (mg/mg).

Samples

Tissue samples were collected from 36 patients in the Otolaryngology Head and Neck Surgery Department of Southern Medical University Zhujiang Hospital from September 2009 to October 2010. There were 20 cases of nasopharyngeal carcinoma, comprising 14 males and six females, of median age 41.8 (range 30–54) years. According to Union for International Cancer Control TNM staging, there were eleven cases of stage II disease, five cases of stage III disease, and four cases of stage IV disease. According to the World Health Organization histologic classification, there were eight cases of moderately differentiated nonkeratinizing squamous cell carcinoma and 12 cases of undifferentiated carcinoma. Tissue samples from eight patients with chronic rhinitis and healthy volunteers were randomly included in the control group. There were 16 cases of glottic carcinoma, comprising

15 males and one female, of median age 61 (range 43–79) years. By TNM staging, there were two cases of stage II disease, seven cases of stage III disease, and seven cases of stage IV disease. There were 12 cases with and four cases without lymph node metastasis. Nontumor tissue samples from corresponding laryngeal resection margins were included as controls. All samples were taken and immediately preserved in liquid nitrogen. All experimental manipulations were done with the approval of the ethics committee of Southern Medical University.

Detection of folate receptors in the tissues of nasopharyngeal and laryngeal carcinomas

To detect FR by immunohistochemistry, fresh frozen specimens were dissected into serial sections about 4 μm thick. Every section was covered on a clean glass slide, dried for approximately 10 minutes, and fixed by 4% polyformaldehyde for 10 minutes at room temperature. Post-fixed sections were washed in phosphate-buffered solution, and soaked in 3% hydrogen peroxide methanol solution (ratio of 30% hydrogen peroxide to pure methanol, 1:50) for 15 minutes to exhaust endogenous peroxide. Each slide was incubated with 5% bovine serum albumin for 20 minutes to block nonspecific antigen sites, and mouse antihuman FR IgG (diluted 1:100 in double-distilled water) was then added. These slides were placed inside a humidified chamber for 30 minutes at room temperature, and were then transferred to a 4°C room overnight. Phosphate-buffered solution was used for the negative control instead of primary antibody and fresh placental tissue was chosen as the positive control. The streptavidin-biotin complex immunocytochemistry protocol was used, and a series of procedures, including staining, mild re-dyeing with hematoxylin, dehydration, coverslipping, and microscope observation, were performed in sequence. The results were considered as positive when claybank particles were observed in the cytoplasm, cell membrane, or nucleus. In accordance with a method reported previously, the proportions of cells positive for FR expression under five high-power microscopic fields were categorized into quartiles, ie, 0%–5% (–), 5%–25% (+), 25%–75% (++), and >75% (+++).

Detection of folate receptors in nasopharyngeal and laryngeal carcinoma cell lines

Nasopharyngeal and laryngeal carcinoma cell lines in logarithmic growth phase were digested with 0.25% trypsin and

washed with phosphate-buffered solution. Next, $5 \times 10^6/\text{mL}$ cell suspensions were prepared and made into cell smear slides. These slides were fixed in ice-cold acetone solution for 10 minutes and dried at room temperature. Post-fixed slides were washed in phosphate-buffered solution, and soaked in 3% H_2O_2 methanol for 15 minutes at room temperature to block the endogenous peroxidases. These slides were then incubated with 5% bovine serum albumin for 20 minutes to block nonspecific antigen sites, with mouse antihuman FR IgG (diluted 1:100 in double-distilled water) added in. Lastly, the slides were placed inside a humidified chamber for 30 minutes at room temperature and then transferred to a 4°C room overnight. Phosphate-buffered solution was used as the negative control instead of primary antibody, and an HeLa cell line with confirmed high FR expression was chosen as the positive control.¹⁹ Each slide was washed in phosphate-buffered solution after incubation with primary antibody. Fluorescein isothiocyanate-conjugated goat antimouse IgG was then added and incubated for 1 hour at 37°C. The slides were washed in phosphate-buffered solution and mounted with DAPI-Fluoromount-G™ (Southern Biotech Associates, Birmingham, AL, USA) for 5 minutes at room temperature. The mounted slides were observed under a fluorescence microscope; positive cells developed green fluorescence located in the cell membrane.

Analysis of CDDP-FA-ASA-MNP in nasopharyngeal and laryngeal carcinoma cells

Prussian blue iron staining

HNE-1 and Hep-2 (FR-expressing) and CNE-2 (not FR-expressing) cells were cultured under standard conditions in nonfolate RPMI-1640 medium for 24 hours, and these three cell lines were then cultured for 6 hours in CDDP-FA-ASA-MNP (final iron concentration 5 $\mu\text{g}/\text{mL}$) diluted with RPMI-1640 medium. After incubation, the culture solution was removed, the cells were washed thoroughly with phosphate-buffered solution and fixed with 4% paraformaldehyde, and then stained with Prussian blue, avoiding light for 30 minutes at room temperature. The nuclei were stained with neutral red, and the slides were observed and photographed under an inverted microscope.

Transmission electron microscopy

As described above, the HNE-1, CNE-2, and Hep-2 cells were incubated for 2 hours with CDDP-FA-ASA-MNP which were diluted with nonfolate RPMI-1640 medium. After incubation, cells were washed with PBS and digested

with 0.25% trypsin. Next, cell suspensions were prepared by PBS. After centrifugation, the cells were fixed by adding 2.5% glutaraldehyde at 4°C and removed the unbound fixative by low-speed centrifugation. The cells were fixed with osmic acid, dehydrated in graded acetone solution, and embedded in epoxy resin. The embedded samples were cut into ultrathin sections and stained with uranyl acetate and lead citrate. The sections were then observed by transmission electron microscopy.

MRI examination of cells in vitro

HNE-1 and CNE-2 cells in logarithmic growth phase were resuspended in phosphate-buffered solution, the concentration of the cell suspension was adjusted to 5×10^4 /mL, and the suspension was then plated into a six-well culture plate (2 mL per well). After adherent growth for 24 hours, the culture solutions were removed. The cells were incubated for 2 hours with CDDP-FA-ASA-MNP which were diluted with nonfolate RPMI-1640 medium. According to iron content, the drug concentrations were 0, 2.5, 5, 10, and 20 μ g/mL. After incubation, the culture solution was removed and the cells were washed thoroughly in phosphate-buffered solution. After digestion with 0.25% trypsin and ceasing digestion with the culture solution comprised of 90% RPMI-1640 and 10% fetal calf serum, the cell solutions were centrifuged to remove the liquid supernatant, resuspended in phosphate-buffered solution, and transferred to a new 15 mL centrifuge tube, to which 2 mL of 1% agarose solution at 37°C was added and mixed in until well distributed. The solution was cooled and formed a solid material at room temperature. Examination of the solid sample was performed using MRI (Quasar Dual 3.0T MR Achieva, Philips, Eindhoven, The Netherlands) with a head coil line in the T2-weighted imaging. Parameters were set as follows: TR/TE (Repetition Time/Echo Time) 3000/80 msec, field of view 180 mm, slice thickness 2.0 mm, and slice distance 1 mm.

Evaluation of targeting properties of CDDP-FA-ASA-MNP in vivo

MRI examination of tumor-bearing nude mice

Four BALB/c nude mice aged 5–7 weeks were purchased from the Animal Experiment Center of Southern Medical University, and raised in a specific pathogen-free environment. The concentration of CNE-2 and HNE-1 cells in logarithmic phase was adjusted to 5×10^7 /mL and 10×10^7 /mL, respectively, and 0.2 mL of each type of cell was then injected subcutaneously into the left and right backside behind the armpit of the nude mouse. When the tumor diameter

reached 8–10 mm, the mice were injected intraperitoneally with 0.2 mL of 5% chloral hydrate to achieve satisfactory anesthesia. After injection, the mice were maintained in the supine position. With the coil covered and placed on the back of the mouse, the first shaft T2-weighted MRI imaging was performed. The mice were injected with 0.2 mL of CDDP-FA-ASA-MNP via the tail vein, and imaged again 24 hours later. Parameters were set as follows: Repetition Time/Echo Time (TR/TE) 2400/74.8 msec, scanning matrix 320×224 , slice thickness 1.0 mm, and slice distance 0.5 mm.

Observation of implanted tumor tissues by Prussian blue iron staining

The mice were euthanized immediately following the second MRI examination. The HNE-1 and CNE-2 tumor masses were dissected from the mice, fixed with 4% paraformaldehyde, embedded in paraffin, cut serially, and stained with Prussian Blue method. In these samples, the distribution of the nanoparticles in tumor tissues were observed by optical microscope.

Statistical analysis

Statistical Package for the Social Sciences version 13.0 software (SPSS Inc, Chicago, IL, USA) was used to analyze all the data. The Chi-square test was used to compare the FR-positive ratio between the head and neck tumor group and the control group. Statistical significance was established at the 5% level ($P < 0.05$) for all statistical analyses.

Results

FR expression in tissue samples of nasopharyngeal and laryngeal carcinoma

Immunohistochemistry revealed that the positive FR expression rate was 85% (17/20) in the nasopharyngeal carcinoma tissue blocks. Among the tissues expressing the FR, eight samples were strongly positive, five were positive, and four were weakly positive (Figure 1A). The positive FR rate in advanced (stage III–IV) nasopharyngeal carcinoma samples (100%) was significantly higher ($P = 0.045$) than in early (stage I–II) samples (72.3%), and there was no significant difference in FR expression between the two pathologic types, ie, differentiated and nondifferentiated nonkeratinizing carcinoma (Table 1). Seven laryngeal carcinoma tissue samples showed strongly positive FR expression, five were positive, and one was weakly positive, and the positive rate of FR in these samples was 81.3% (13/16, Figure 1B). The positive rate of FR in advanced (stage III–IV) laryngeal carcinoma

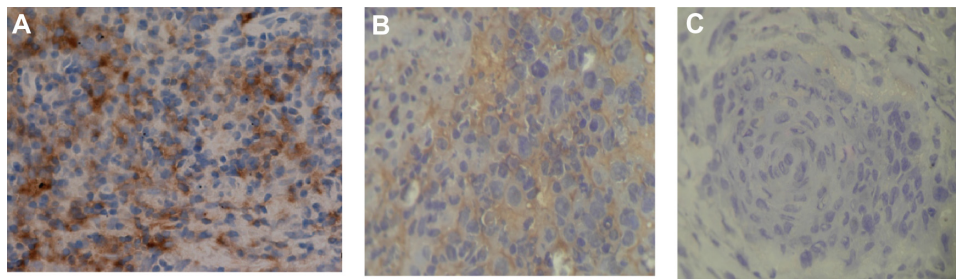


Figure 1 State of folate receptor expression in different tissues. **(A)** Strongly positive expression of folate receptor in a nasopharyngeal carcinoma tissue sample. **(B)** Strongly positive folate receptor expression in a laryngeal carcinoma tissue sample. **(C)** Negative expression of folate receptor in normal tissue sample next to laryngeal carcinoma tissue, $\times 200$.

samples (92.9%, 13/14) was much higher ($P = 0.025$) than in early (stage I–II) disease (0%, 0/2) and was also much higher ($P = 0.007$) in samples from patients with lymph node metastases (N_{1-2} , 100%) than from patients without (N_0 , 25%), both with a significant difference (Table 2). FR expression was not associated with gender or age in either nasopharyngeal or laryngeal carcinoma ($P > 0.05$). The FR was found neither in normal nasopharynx tissues (0/8) nor in normal tissues adjacent to the laryngeal carcinomas (0/16). The difference between normal and carcinoma tissues was highly significant ($P < 0.01$).

Folate receptor expression in cultured cells

Immunofluorescence showed that only two of the seven cell lines, ie, HNE-1 and Hep-2, were strongly positive for FR. The rate of FR positivity in the HNE-1 cell line was 93.7% and for Hep-2 was 90.4%. The other five cell lines did not express the FR (Figure 2).

Table 1 Relationship between expression of the folate receptor, clinical characteristics, and pathologic types of nasopharyngeal carcinoma

Clinical characteristics	n	Folate receptor		P value
		Positive	Negative	
Gender				
Male	14	12 (85.7%)	2 (14.3%)	0.891
Female	6	5 (83.3%)	1 (16.7%)	
Age, years				
<40	9	8 (88.9%)	1 (11.1%)	0.660
≥ 40	11	9 (81.8%)	2 (18.2%)	
Clinical stage				
I–II	11	8 (72.3%)	3 (27.7%)	0.045
III–IV	9	9 (100%)	0	
Pathological types				
Differentiated	8	7 (87.5%)	1 (12.5%)	0.798
Undifferentiated	12	10 (83.3%)	2 (16.7%)	

Uptake of CDDP-FA-ASA-MNP by nasopharyngeal and laryngeal carcinoma cells

Nasopharyngeal and laryngeal carcinoma cells were cocultured for 6 hours with CDDP-FA-ASA-MNP containing 5 $\mu\text{g/mL}$ iron. The results of iron staining and electron microscopy showed that HNE-1 and Hep-2 cells both took up CDDP-FA-ASA-MNP, while CNE-2 cells did not (Figures 3 and 4). From MRI T2-weighted images of HNE-1 and CNE-2 cells, which had been cultured with different concentrations of CDDP-FA-ASA-MNP for 2 hours, we observed decreased signals compared with the control group. With the increasing concentration of drug, the signal of HNE-1 cells receded gradually but distinctly, whereas under the same conditions, the signal from CNE-2 cells receded only a little. The reduction of the signal in CNE-2 cells with a maximum dose of the drug was similar with HNE-1 cells with a minimum dose (Figure 5).

Table 2 Relationship between folate receptor expression and clinical characteristics of patients with laryngeal carcinoma

Clinical characteristics	n	Folate receptor		P-value
		Positive	Negative	
Gender				
Male	15	12 (80%)	3 (20%)	1.000
Female	1	1 (100%)	0	
Age, years				
<61	8	6 (75%)	2 (25%)	1.000
≥ 61	8	7 (87.5%)	1 (12.5%)	
Clinical stage				
I	2	0	2 (100%)	0.025
III–IV	14	13 (92.9%)	1 (7.1%)	
Lymph node metastasis				
N_0	4	1 (25%)	3 (87.5%)	0.007
N_{1-2}	12	12 (100%)	0	

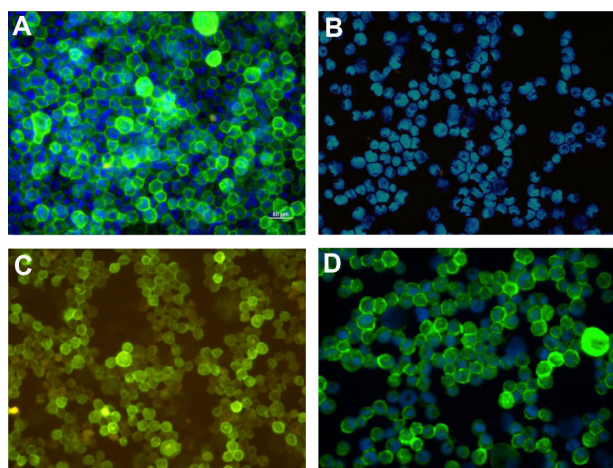


Figure 2 Folate receptor expression in cultured cells. (A) HNE-1, FR-positive, $\times 400$, (B) CNE-2 FR-negative, $\times 200$, (C) Hep-2, FR-positive, $\times 200$, and (D) HeLa, FR-positive, $\times 400$.

Abbreviation: FR, folate receptor.

CDDP-FA-ASA-MNP targeting in vivo

After treatment with CDDP-FA-ASA-MNP, the MRI T2-weighted images of HNE-1 transplanted tumors in the nude mice showed low signal intensity, while CNE-2 tumors did not show this feature (Figure 6). Iron staining revealed that cells in the HNE-1 transplanted tumors took up many blue dyed nanoparticles, while those in the CNE-2 tumors did not (Figure 7).

Discussion

Nasopharyngeal and laryngeal carcinomas are the most common head and neck malignancies in south China. The majority of these tumors are squamous cell carcinomas and have a high rate of metastasis. Nowadays, chemotherapy has become an important treatment for patients with head and neck carcinoma, especially for those with advanced nasopharyngeal carcinoma. After injection into the vessels, the chemotherapeutic drug distributes widely throughout the body, into both tumor tissue and normal tissue. To ensure a therapeutic antitumor effect, high doses should be used,

which inevitably produce severe systemic toxicity. Targeting chemotherapy specifically to the tumor site can selectively kill cancer cells using lower systemic doses and reducing side effects. In recent years, molecular targeted therapy has become increasingly important in the treatment of advanced tumors. A targeted therapeutic strategy can not only improve the therapeutic effect of anticancer drugs, but can also reduce the dosage needed and thereby minimize side effects. The epidermal growth factor receptor and vascular endothelial growth factor have already been used as molecular targets in clinical anticancer therapy.^{20,21}

In our study, FR was detected in 85% of primary nasopharyngeal carcinomas and 81.3% of laryngeal carcinomas, with nearly half of these cases having a strongly positive FR expression level. We found the highest FR level in advanced tumors and in cases with lymph node metastases, but negative FR expression in normal nasopharyngeal and laryngeal tissues and normal adjacent mucosa. These results are consistent with those reported by other researchers for endometrial, lung, and other cancers.^{22,23} We detected FR expression in six nasopharyngeal carcinoma cell lines and found that the HNE-1 cell line has the highest FR expression level, with 93.7% of cells being positive for FR. The HNE-1 cell line came from a highly tumorigenic, Epstein-Barr virus-positive, squamous cell nasopharyngeal carcinoma. We did not detect FR expression in the other five nasopharyngeal carcinoma cell lines, ie, CNE-1, CNE-2, HNE-2, SUNE-1, and 5-8F. These results are inconsistent with the high FR expression levels found in the clinical cases of nasopharyngeal carcinoma. We speculate that certain genetic traits of these immortalized nasopharyngeal carcinoma cell lines had changed during long periods of in vitro culture. We found that FR was highly expressed in Hep-2 laryngeal cancer cells, with a positivity rate of 90.4%. The FR is expressed in a significant proportion of primary head and neck malignancies and corresponding lymph node metastases, and correlates with a worse

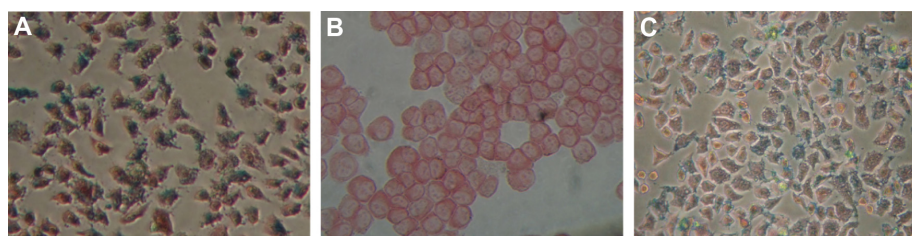


Figure 3 Iron staining results for cultured cells taking in CDDP-FA-ASA-MNP. (A) HNE-1, FR-positive cytoplasm in which scattered blue dyed particles were found. (B) CNE-2, FR-negative cytoplasm which did not contain blue particles. (C) Hep-2, FR-positive cytoplasm in which scattered blue dyed particles were found. The iron concentration in the drug was 5 $\mu\text{g}/\text{mL}$, $\times 200$.

Abbreviations: CDDP-FA-ASA-MNP, folate-conjugated cisplatin-loaded magnetic nanoparticles; FR, folate receptor.

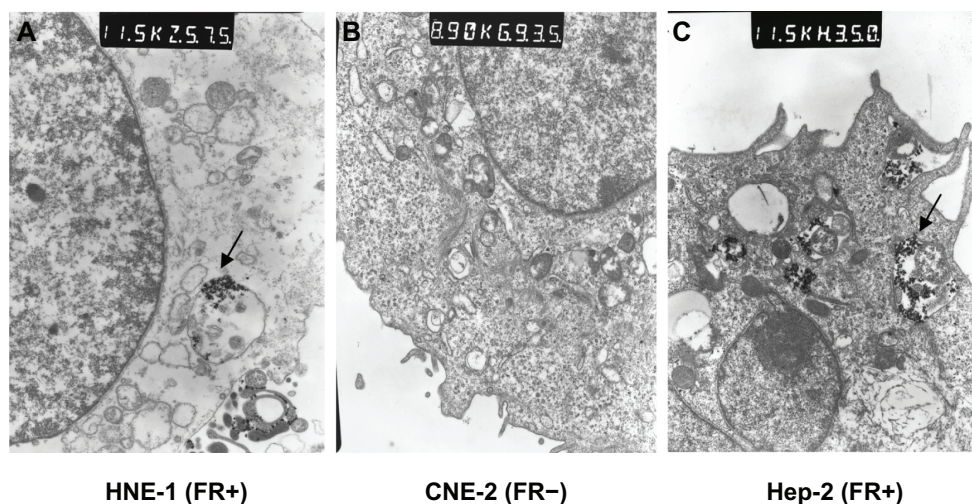


Figure 4 Electron microscopic image of cultured cells taking in CDDP-FA-ASA-MNP. (A) Arrow shows a pinocytotic bubble containing magnetic nanoparticles found in the cytoplasm of an HNE-1 cell, 115,000 \times . (B) No nanoparticles in the cytoplasm of CNE-2, 89,000 \times . (C) Arrow shows a pinocytotic bubble containing magnetic nanoparticles found in the cytoplasm of a Hep-2 cell, 115,000 \times .

Abbreviation: CDDP-FA-ASA-MNP, folate-conjugated cisplatin-loaded magnetic nanoparticles.

clinical outcome. These findings provide support for FR-mediated nanotherapeutics in squamous cell carcinoma of the head and neck.

Magnetic nanoparticles not only have the common characteristics of nanosized particles, including small particle diameters, large specific surface area, and special surface effects, but also have superparamagnetic properties, which can induce directional movement under a magnetic field.²⁴ In previous research, we developed superparamagnetic cisplatin-loaded magnetic nanoparticles.^{25,26} This nanomedicine is magnetically targeted, and has high security and good drug-loading performance,^{27–29} but is deficient in targeting properties at the cell level.³⁰ We prepared CDDP-FA-ASA-MNP,¹⁸ which have potential FR molecular targeting characteristics and improved targeted drug delivery at the cell level.

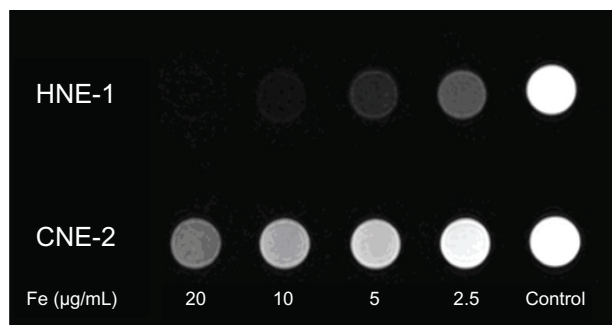


Figure 5 Magnetic resonance T2-weighted images of HNE-1 and CNE-2 cells which had been cultured in vitro with different concentrations of CDDP-FA-ASA-MNP for 2 hours. Fe ($\mu\text{g/ml}$) refer to the iron concentration of CDDP-FA-ASA-MNP solution. **Abbreviation:** CDDP-FA-ASA-MNP, folate-conjugated cisplatin-loaded magnetic nanoparticles.

With a Fe_3O_4 core, the magnetic nanoparticles can be detected conveniently by several methods, ie, Prussian blue staining, MRI, and transmission electron microscopy, not only in vitro but also in vivo. In this way, the distribution of this magnetic nanomedicine has been researched. We added FR-targeted magnetic nanomedicines to a culture system of FR-positive HNE-1 and Hep-2 cells and FR-negative CNE-2 cells. A large number of nanoparticles were found in the HNE-1 and Hep-2 cells by Prussian blue staining and examination by transmission electron microscopy, but no nanoparticles were seen in CNE-2 cells. This result indicates that the nanoparticles inside the cells were primarily taken up through FR-mediated endocytosis. Cocultured with the CDDP-FA-ASA-MNP for 2 hours, MRI images were gained for HNE-1 and CNE-2 cell suspensions. The MRI T2-weighted image intensity of HNE-1 cells treated with FR-targeted nanoparticles decreased significantly. In contrast, the T2 signal did not show an obvious decrease for CNE-2 cells treated in the same way. The MRI signal intensity of cells incubated with the FR-targeted nanoparticles decreased to varying degrees in T2-weighted images depending on the Fe_3O_4 concentration in the cells. This decrease in signal intensity was significant when the amount of intracellular Fe_3O_4 particles was higher. This result indicates that FR-positive HNE-1 cells had taken in more nanoparticles by FR-mediated endocytosis than had FR-negative CNE-2 cells.

This cisplatin-loaded FR targeted nanomedicine also showed specific distribution in vivo. Using two groups of nude mice with nasopharyngeal carcinoma xenografts, the

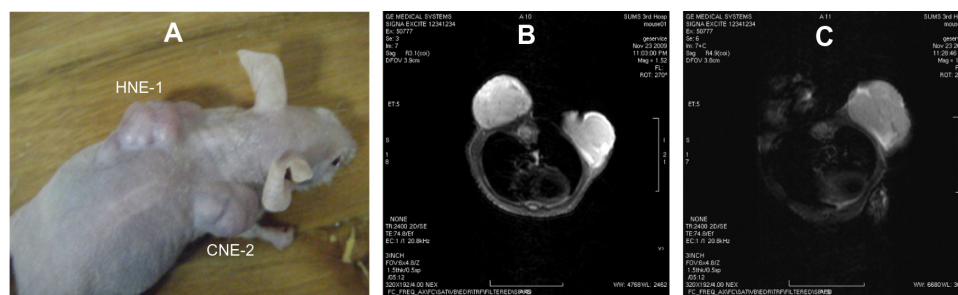


Figure 6 Magnetic resonance images of transplanted tissue in nude mice. **(A)** Mouse bearing two kinds of tumor at the same time, **(B)** T2-weighted image before treatment with CDDP-FA-ASA-MNP, and **(C)** T2-weighted image 24 hours after treatment. The HNE-1 tumor shows a reduction in signal intensity.
Abbreviation: CDDP-FA-ASA-MNP, folate-conjugated cisplatin-loaded magnetic nanoparticles.

FR-targeted nanomedicine was injected into each animal via the tail vein. Twenty-four hours later, MRI T2-weighted images showed that the signal intensity of the HNE-1 tumor area had decreased unevenly. The peripheral portion of the HNE-1 xenograft tumor showed a greater decrease in intensity than the central portion. This phenomenon may be due to the peripheral area having more blood vessels, while the necrotic tissue is obviously found in the central area of a large tumor. However, no significant change in MRI T2-weighted image signal intensity was seen in the CNE-2 xenograft tumors after injection. We also found more Fe_3O_4 nanoparticles distributed in HNE-1 xenograft tumor tissue than in CNE-2 tumors by Prussian blue staining. This result further suggests that this FR-targeted magnetic nanomedicine can be specifically unclaimed by FR-positive HNE-1 nasopharyngeal carcinoma cells.

Conclusion

Our immunohistochemistry and immunofluorescence data indicate that nasopharyngeal and laryngeal squamous cell carcinoma tissues and HNE-1 and Hep-2 cell lines have high expression of FR and that normal tissues express very little FR. We have prepared CDDP-FA-ASA-MNP for anticancer

therapy. This targeted nanomedicine can be taken up into FR-positive tumor cells by FR-mediated endocytosis. Our preliminary study has shown that targeted drug delivery is a highly desirable strategy to improve diagnostic imaging and the therapeutic outcome by a combination of enhanced efficacy and reduced systemic toxicity. These FR-targeted nanoparticles demonstrate potential as a powerful multifunctional platform for drug delivery and gene vector applications in the future treatment of head and neck tumors.

Acknowledgment

This work was supported by grants from the Guangdong Natural Science Foundation of China (10251051501000001), the Specialized Research Fund for the Doctoral Program of Higher Education from the Ministry of Education of China (20114433110001), and Foundation for Distinguished Young Talents in Higher Education of Guangdong, People's Republic of China (LYM09036). The authors thank Gemane Starck for English language revision.

Disclosure

The authors report no conflicts of interest in this work.

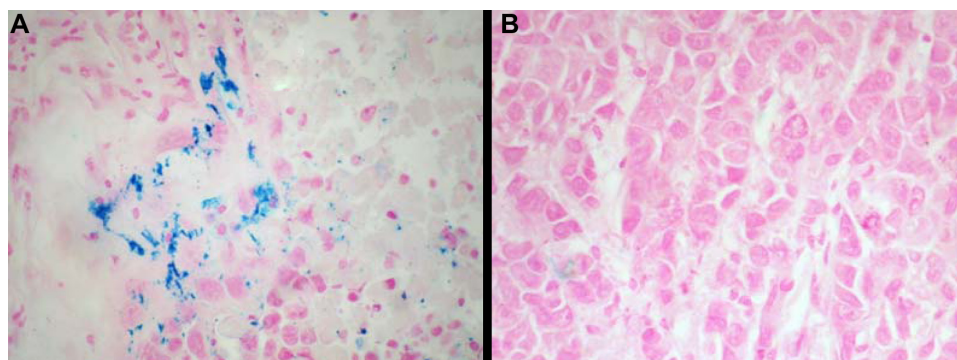


Figure 7 Iron staining of transplanted tumor on nude mice after 24-hour CDDP-FA-ASA-MNP treatment; **A**, Cells of HNE-1 transplant tumors containing blue dyed particles; **B**, Cells of CNE-2 tumors containing free of particles. $\times 400$

References

- Parker N, Turk MJ, Westrick E, Lewis JD, Low PS, Leamon CP. Folate receptor expression in carcinomas and normal tissues determined by a quantitative radioligand binding assay. *Anal Biochem.* 2005;338(2):284–293.
- Elnakat H, Ratnam M. Distribution, functionality and gene regulation of folate receptor isoforms: implications in targeted therapy. *Adv Drug Deliv Rev.* 2004;56(8):1067–1084.
- Salazar MD, Ratnam M. The folate receptor: what does it promise in tissue-targeted therapeutics? *Cancer Metastasis Rev.* 2007;26(1):141–152.
- Hartmann LC, Keeney GL, Lingle WL, et al. Folate receptor overexpression is associated with poor outcome in breast cancer. *Int J Cancer.* 2007;121(5):938–942.
- Dainty LA, Risinger JJ, Morrison C, et al. Overexpression of folate binding protein and mesothelin are associated with uterine serous carcinoma. *Gynecol Oncol.* 2007;105(3):563–570.
- Kalli KR, Oberg AL, Keeney GL, et al. Folate receptor alpha as a tumor target in epithelial ovarian cancer. *Gynecol Oncol.* 2008;108(3):619–626.
- Leamon CP, Reddy JA. Folate-targeted chemotherapy. *Adv Drug Deliv Rev.* 2004;56(8):1127–1141.
- Fani M, Tamma ML, Nicolas GP, et al. In vivo imaging of folate receptor positive tumor xenografts using novel ⁶⁸Ga-NODAGA-folate conjugates. *Mol Pharm.* 2012;9(5):1136–1145.
- Al Jammaz I, Al-Otaibi B, Amer S, Al-Hokbany N, Okarvi S. Novel synthesis and preclinical evaluation of folic acid derivatives labeled with (18)F-[FDG] for PET imaging of folate receptor-positive tumors. *Nucl Med Biol.* 2012;39(6):864–870.
- Al Jammaz I, Al-Otaibi B, Amer S, Okarvi SM. Rapid synthesis and in vitro and in vivo evaluation of folic acid derivatives labeled with fluorine-18 for PET imaging of folate receptor-positive tumors. *Nucl Med Biol.* 2011;38(7):1019–1028.
- Liang B, He ML, Xiao ZP, et al. Synthesis and characterization of folate-PEG-grafted-hyperbranched-PEI for tumor-targeted gene delivery. *Biochem Biophys Res Commun.* 2008;367(4):874–880.
- Duarte S, Faneca H, Lima MC. Folate-associated lipoplexes mediate efficient gene delivery and potent antitumoral activity in vitro and in vivo. *Int J Pharm.* 2012;423(2):365–377.
- Saba NF, Wang X, Müller S, et al. Examining expression of folate receptor in squamous cell carcinoma of the head and neck as a target for a novel nanotherapeutic drug. *Head Neck.* 2009;31(4):475–481.
- Wang X, Li J, Wang Y, et al. HFT-T, a targeting nanoparticle, enhances specific delivery of paclitaxel to folate receptor-positive tumors. *ACS Nano.* 2009;3(10):3165–3174.
- Dosio F, Arpico S, Stella B, Brusa P, Cattel L. Folate-mediated targeting of albumin conjugates of paclitaxel obtained through a heterogeneous phase system. *Int J Pharm.* 2009;382(1–2):117–123.
- Hong G, Yuan R, Liang B, Shen J, Yang X, Shuai X. Folate-functionalized polymeric micelle as hepatic carcinoma-targeted, MRI-ultrasensitive delivery system of antitumor drug. *Biomed Microdevices.* 2008;10(5):693–700.
- Ward BB, Dunham T, Majoros IJ, Baker JR Jr. Targeted dendrimer chemotherapy in an animal model for head and neck squamous cell carcinoma. *J Oral Maxillofac Surg.* 2011;69(9):2452–2459.
- Xie M, Xu Y, Liu J, Zhang T, Zhang H. Preparation and characterization of folate targeting magnetic nanomedicine loaded with cisplatin. *J Nanomater.* 2012;2012:921034.
- Zhang Q, Zhang Y, Yang Y, Xiang G. Specific binding of folate conjugated PGA to FR-positive tumor cells. *Chinese Pharmacological Bulletin.* 2007;23(6):746–750.
- Razak AR, Siu LL, Le Tourneau C. Molecular targeted therapies in all histologies of head and neck cancers: an update. *Curr Opin Oncol.* 2010;22(3):212–220.
- Goerner M, Seiwert TY, Sudhoff H. Molecular targeted therapies in head and neck cancer. *Head Neck Oncol.* 2010;2:8.
- Iwakiri S, Sonobe M, Nagai S, Hirata T, Wada H, Miyahara R. Expression status of folate receptor alpha is significantly correlated with prognosis in non-small-cell lung cancers. *Ann Surg Oncol.* 2008;15(3):889–899.
- Allard JE, Risinger JJ, Morrison C, et al. Overexpression of folate binding protein is associated with shortened progression-free survival in uterine adenocarcinomas. *Gynecol Oncol.* 2007;107(1):52–57.
- Kim DK, Zhang Y, Voit WK, Raob V, Muhammeda M. Synthesis and characterization of surfactant-coated superparamagnetic monodispersed iron oxide nanoparticles. *J Magn Mater.* 2001;225(1–2):30–36.
- Xu XQ, Shen H, Xu JR, Xie MQ, Li XJ. The colloidal stability and core-shell structure of magnetite nanoparticles coated with alginate. *Appl Surf Sci.* 2006;253(4):2158–2164.
- Xie M, Chen S, Xu X, Li Z, Shen H, Xie J. Preparation of two kinds of superparamagnetic carriers-supported cis-platinum-complexes and the comparison of their characteristics. *Chin Sci Bull.* 2006;51(2):151–157.
- Chen S, Xie M, Wang L, Long Z, Li Z, Zhang H. Safety assessment of modified cisplatin magnetic nanomedicine. *China Pharmacy.* 2008;19(25):1941–1943.
- Xie M, Wang L, Chen S, Xu X, Shen H. Tissue distribution of cisplatin-loaded magnetic nanomedicine in mice. *Chinese Pharmaceutical Journal.* 2010;45(21):1644–1647.
- Huang S, Xie M, Li Y, Yuan X, Chen S. An experimental study of the distribution and targeting effect of CDDP-loaded magnetic nanoparticles in nude mice with transplanted nasopharyngeal carcinoma. *J Med Res.* 2011;40(2):22–26.
- Long Z, Xie M, Zhang T, Shen H, Xu X, Guo L. Effect of targeted therapy with cisplatin-loaded magnetic nanoparticles combined with radiotherapy for nasopharyngeal carcinoma in nude mice. *Nan Fang Yi Ke Da Xue Xue Bao.* 2009;29(9):1827–1830. Chinese.

International Journal of Nanomedicine

Publish your work in this journal

The International Journal of Nanomedicine is an international, peer-reviewed journal focusing on the application of nanotechnology in diagnostics, therapeutics, and drug delivery systems throughout the biomedical field. This journal is indexed on PubMed Central, MedLine, CAS, SciSearch®, Current Contents®/Clinical Medicine,

Submit your manuscript here: <http://www.dovepress.com/international-journal-of-nanomedicine-journal>

Dovepress

Journal Citation Reports/Science Edition, EMBase, Scopus and the Elsevier Bibliographic databases. The manuscript management system is completely online and includes a very quick and fair peer-review system, which is all easy to use. Visit <http://www.dovepress.com/testimonials.php> to read real quotes from published authors.